Bioorganic Chemistry 94 (2020) 103421

Contents lists available at ScienceDirect

Bioorganic Chemistry

journal homepage: www.elsevier.com/locate/bioorg

Synthesis and biological evaluation of new chloro/acetoxy substituted isoindole analogues as new tyrosine kinase inhibitors

Aytekin Köse[a], Meltem Kaya[b], Nurhan H. Kishalı[c], Atilla Akdemir[d], Ertan Şahin[c], Yunus Kara[c,*], Gülşah Şanlı-Mohamed[b,*]

[a] Department of Chemistry, Faculty of Sciences and Letters, Aksaray University, 68100 Aksaray, Turkey
[b] Department of Chemistry, Faculty of Sciences, İzmir Institute of Technology, 35430 İzmir, Turkey
[c] Department of Chemistry, Faculty of Sciences, Ataturk University, 25240 Erzurum, Turkey
[d] Computer-Aided Drug Discovery Laboratory, Department of Pharmacology, Faculty of Pharmacy, Bezmialem Vakif University, 34093 Istanbul, Turkey

ARTICLE INFO

Keywords:
Norcantharimides
Isoindole
Cytotoxicity
HeLa cells

ABSTRACT

We have developed a versatile synthetic approach for the synthesis of new isoindole derivatives via the cleavage of ethers from tricyclic imide skeleton compounds. An *exo*-cycloadduct prepared from the Diels–Alder reaction of furan and maleic anhydride furnished imide derivatives. The epoxide ring was opened with Ac_2O or Ac_2O/AcCl in the presence of a catalytic amount of H_2SO_4 in order to yield new isoindole derivatives **8a-d** and **9a-d**. The anticancer activity of these compounds was evaluated against the HeLa cell lines. The synthesized compounds showed inhibitory effects on the viability of HeLa cells and the degree of cytotoxicity was increased with the level of bigger branched isoindole derivatives. To better understand the acting mechanism of these molecules, western blot analysis was performed with using mTOR and its downstream substrates. In addition, human mTOR and ribozomal S6 kinase β1 (RS6Kβ1) have been investigated with molecular modelling studies as possible targets for compound series **8** and **9**.

1. Introduction

The norcantharimides are known as 3a,4,7,7a-tetrahydro-1*H*-4,7-epoxyisoindole-1,3(2*H*)-dione derivatives, as shown in Fig. 1. Two methods are generally used to derive norcantharimide or isoindole derivatives. Various substituted groups are bonded to the nitrogen atom in the imide ring or to any atom in the cyclohexane ring.

In recent years, the biological significance of different *N*-substituted isoindole-1,3-dione derivatives has been investigated by various research groups [1–7]. One class of *N*-substituted isoindole-1,3-dione derivatives contains the norcantharimides, which also have potential cytotoxic effects [2,4].

The anticancer activities of a great deal of isoindole-1,3-dione derivatives have been studied in various cell lines, such as human liver carcinoma cell lines (HepG2, Hep3B, and SK-HEP-1), a bladder cancer cell line (BFTC905), epithelial cells, human lung adenocarcinoma (A549), Caucasian promyelocytic leukemia cells (HL-60), a human breast adenocarcinoma cell line (MCF-7), and colon carcinoma cell line SW480 [5–9]. McCluskey et al. reported the anticancer activity of different groups related to the imide nitrogen in isoindole-1,3-dione [5–9]. The norcantharimides or isoindole-1,3-dione are known to interact with protein phosphatases such as PP1 and PP2A. The anticancer activity of norcantharimides is believed to be due to the inhibition of protein phosphatase 1 and protein phosphatase 2A. Recently, researchers have been exploring the connection between the protein phosphatase inhibitor and the anticancer activity [6–11].

In our previous papers we described a facile synthesis of isoindoline-1,3-dione derivatives 3 from 3-sulfolene [12]. Unlike other synthetic methods, we developed the synthesis of a new class of isoindole derivatives containing substituted groups on the cyclohexane ring. More recently, we synthesized novel isoindole derivatives and examined their antiproliferative properties in cell lines MCF-7 (breast adenocarcinoma) and A549 (human alveolar basal epithelial adenocarcinoma) [13]. The results demonstrated here suggest that these new compounds might be considered as possible potential anticancer agents for the treatment of lung and breast cancer.

In light of these findings, we decided to develop an alternative strategy for the synthesis of chlorine- and acetate-substituted isoindole derivatives. Herein, we report the synthesis and evaluation of cytotoxicities of isoindole derivatives containing chlorine atom and acetate functional groups against human cervical carcinoma cells.

* Corresponding authors at: Izmir Institute of Technology, Science Faculty, Department of Chemistry, Urla, Izmir, Turkey (G.Ş. Mohamed).
E-mail addresses: yukara@atauni.edu.tr (Y. Kara), gulsahsanli@iyte.edu.tr (G. Şanlı-Mohamed).

https://doi.org/10.1016/j.bioorg.2019.103421
Received 13 August 2019; Received in revised form 23 September 2019; Accepted 2 November 2019
Available online 04 November 2019
0045-2068/

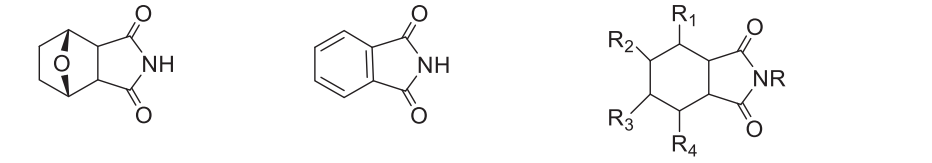

Fig.1. The structure of norcantharimide (**1**), isoindoline-1,3-dione (**2**), and isoindoline-1,3-dione derivatives **3**.

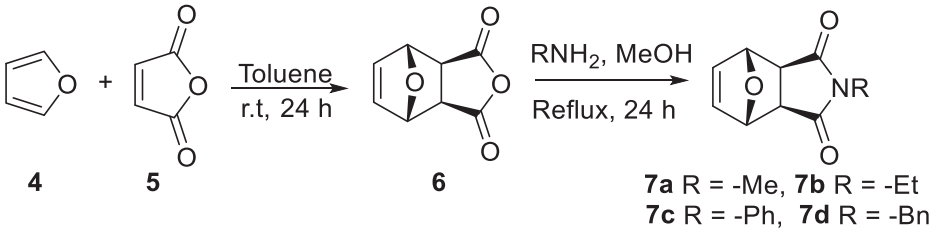

Scheme 1. Synthesis of tricyclic imides **7a-d.**

2. Result and discussion

2.1. Chemistry part

For the synthesis of norcantharimide derivatives, 3a,4,7,7a-tetrahydro-4,7-epoxyisobenzofuran-1,3-dione **(6)** was used as the key compound. This key compound was prepared *via* an *exo*-selective cycloaddition of furan and maleic anhydride (Scheme 1) [13–15]. The reaction of the appropriate primer amine with epoxyisobenzofuran-1,3-dione **6** in the presence of MeOH gave the tricyclic imides in 54–90% yield **7a-d** (Scheme 1). Through the use of four different primary amines under the same reaction conditions we were able to synthesize corresponding imides **7a-d**.

In our previous paper we described a facile synthesis of 2-alkyl-1,3-dioxo-2,3,3a,4,7,7a-hexahydro-1*H*-isoindole-4,7-diyl diacetate from tricyclic imides **7a** by cleavage of ethers from tricyclic imide skeletal compounds [13]. In this work, treatment of tricyclic imides **7a-d** with acetic anhydride in the presence of H_2SO_4 at room temperature gave *trans*-diacetate derivatives of isoindole-1,3-dione **8a-d** as a sole product in a yield of 57–82%. In this reaction, the etheric bond is cleaved stereospecifically to give *trans*-diacetate **8a**. Furthermore, a series of tricyclic imides were prepared in order to obtain *trans*-diacetate derivatives. Under the same reaction conditions, *trans*-acetate derivatives **8b-d** were obtained from the cleavage of ethers of prepared tricyclic imides **7b-d** (Scheme 2).

Based on this reaction, we decided to synthesize chlorine- and acetate-substituted isoindole derivatives. For this purpose, we used acetyl chloride in the presence of H_2SO_4 for the cleavage of ethers. Treatment of tricyclic imide **7a** with acetyl chloride in the presence of H_2SO_4 in acetic anhydride at room temperature gave chloroacetate isoindole **9a** as the sole product in a yield of 67%. We expected formation of 7-chloro-2-methyl-1,3-dioxo-2,3,3a,4,7,7a-hexahydro-1*H*-isoindol-4-yl acetate by the H_2SO_4-assisted ring opening of **7a**. However, the rearrangement product 4-acetoxy-5-chloroisoindole derivative **9a** was formed in the presence of acetyl chloride in this reaction (Scheme 3).

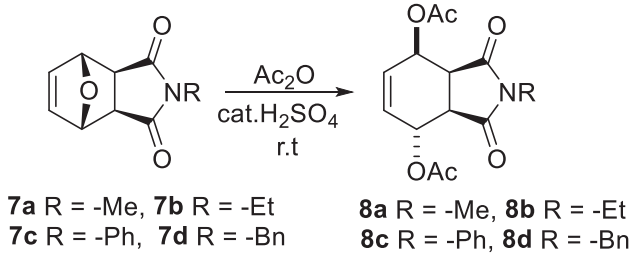

Scheme 2. Synthesis and conditions of compounds **8a-d.**

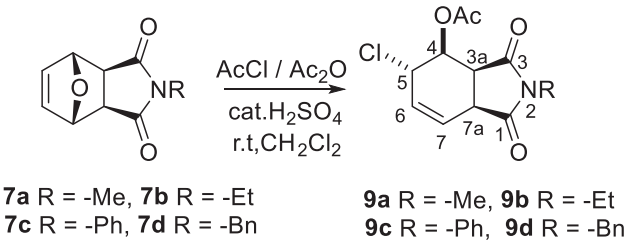

Scheme 3. Synthesis and conditions of compounds **9a-d.**

The most conspicuous features in the ^{1}H NMR spectrum of chloroacetate **9a** were the presence of the double bond protons and incorporation of the chlorine atom in the molecule. Double resonance experiments clearly indicated that the HC═CH double bond was located between the carbon atoms bearing chlorine atom C(5) and bridgehead carbon C(7a). Furthermore, ^{1}H NMR analysis of the crude product suggested that chloroacetate **9a** was a single stereoisomer, although two stereoisomers would be formed. The exact stereochemistry of the chlorine atom in **9a** was confirmed by single-crystal X-ray analysis of chloroacetate **9a** (Fig. 2).

Compound **9a** crystallizes in the monoclinic space group C2/c with two molecules in the asymmetric unit and each one has the same stereochemistry. The *cyclohexene* unit has the half-chair conformation; C—C (*cyclohexene*) distances are in the range of 1.485(4)-1.530(4) Å and all have the single bond character. The C2═C3 double bond in the *cyclohexene* unit is 1.310(4) Å, the pyrrolidine unit has an envelope conformation, and C—N bond lengths are in the range of 1.372(4)-1.382(4) Å. The C4—Cl1 bond distance is 1.800(3) Å. The structure contains four asymmetric carbon atoms and the stereogenic centers are as follows: C1(*R*), C4(*R*), C5(*R*), C6(*R*). In the solid state, compound **9a** is stabilized via numerous intermolecular C—H···O [*D*···*A* = 3.264(3)-3.507 Å] interactions, which leads to the formation of a polymeric structure. Along with that, C—H···Cl [*D*···*A* = 3.487(4) Å] interactions have a contribution in the formation of a stable structure (Fig. 2b).

The regio- and stereoselective formation of product **9a** is remarkable. We suppose that the formation of product **9a** from **8a** proceeds by S_N2' reactions [16] as outlined in Scheme 4.

In the first step, tricyclic imide converts to diacetate in the presence of acetyl chloride in acetic anhydride. The free chloride ion (Cl^-) is also formed during this reaction. The S_N2' reaction with Cl^- can then occur at C(5) on the *syn*-face with respect to the acetoxy group (in acidic medium) in the allylic position at C(7) to give chloroacetate **9a**. Furthermore, the X-ray of structure **9a** can inform us about the approach of the chloride ion (Cl^-). The X-ray crystal structure indicates clearly that the chloride ion approaches the double bond in **8a**

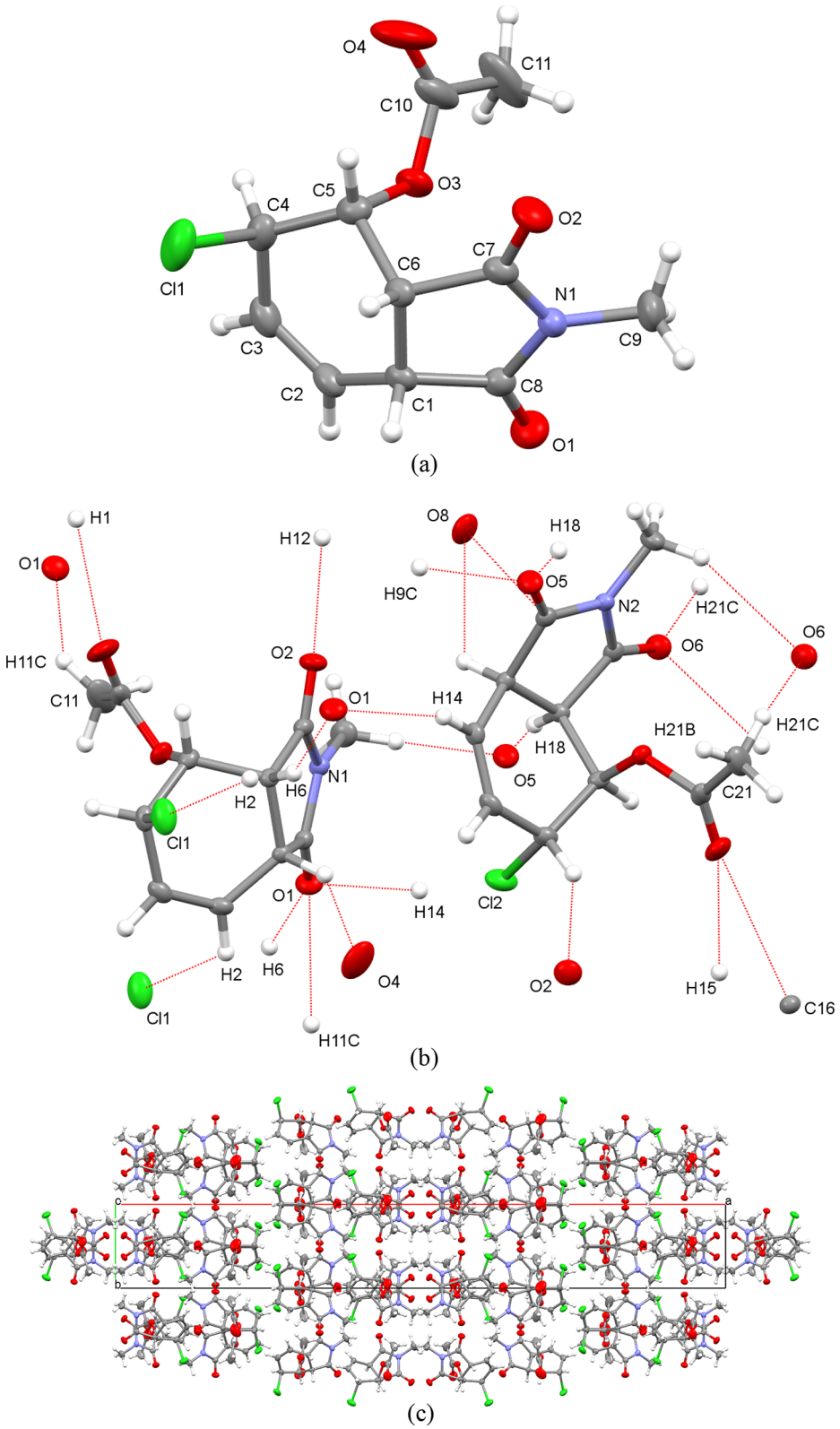

Fig. 2. (a) Crystal structure of compound **9a** with atom labeling scheme (thermal ellipsoids are drawn at the 40% probability level). (b) Intermolecular interactions of **9a** indicated by dotted lines. There are two molecules in the asymmetric unit and the circumference of each is different. (c) Unit cell with the packing of the molecules in the crystal.

exclusively from the sterically less crowded face with respect to the imide ring of the molecule and this leads to *trans*-chloroacetate **9a**. To support the proposed reaction mechanism, we carried out another experiment with tricyclic imide **7a** for a better understanding of the reaction. The reaction mixture was monitored by recording ^{1}H NMR spectra at four different times. As the halogenation reaction proceeded, monitoring of the product ratio by NMR showed an increase in the signals corresponding to chloroacetate **9a** over the course of time. On

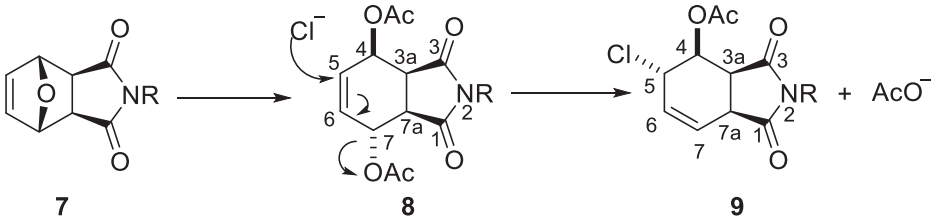

Scheme 4. The proposed mechanism for the synthesis of 4-acetoxy-5-chloroisoindole derivative **9.**

the basis of this observation, the reaction proceeds first with protonation followed by attack of the free chloride to substitute the acyl group. After this promising result, a series of tricyclic imides were prepared in order to obtain *trans*-chloroacetate derivatives. Under the same reaction conditions, *trans*-chloroacetate derivatives **9b-d** were obtained by acetylation followed by displacement reaction (Scheme 3).

2.2. Biological evaluation

Cytotoxic effects of all newly synthesized compounds (drugs) on HeLa cells were determined and IC_{50} values of those drugs were calculated using the MTT activity assay. Cell viability of HeLa cells using all seven compounds was followed for 24, 48, and 72 h of incubation time. According to the results of these experiments, the optimum incubation period was determined as 48 h. Some compounds, and especially **9c**, were not effective against HeLa cells when incubated for 24 h. This might be related to the dissolution of the drug in the cell medium and transportation into the cell. In 2015, Mondal et al. used 1-amino-4-hydroxy-9,10-anthraquinone on MDA-MB-231 breast adenocarcinoma cells; they reported 50% inhibitory rates of this molecule as 200 μM for 24 h of incubation and 140 μM for 48 h of incubation [17]. In another study, 3-isobutylhexahydropyrrolo [1,2-*a*]pyrazine-1,4-dione (PPDHMP), which was extracted from a new marine bacterium called *Staphylococcus* sp. strain MB30, was used on A549 (lung cancer cells), HeLa (cervical cancer cell line), and normal peripheral blood mononuclear cells (PBMCs). PPDHMP was used at various concentrations (1, 10, 25, 50, and 100 μg/mL) for 6, 12, 18, and 24 h of incubation. It showed no toxic effects on PBMCs, but it had 19.94 μg/mL IC_{50} on HeLa cells and 16.73 μg/mL IC_{50} on A549 cells for 24 h of incubation. The most effective inhibition was observed with 24 h of incubation in that research [18].

On the other hand, when drugs were incubated for 72 h, **9a** and **8b** in particular lost their stability/effectiveness, and cells might become more resistant to drugs after long incubation periods. In 2003, Mai and his co-workers investigated the effect of pyrrole-C(2) and -C(4) substitutions on biological activity and they reported some molecules (compounds **3a** and **1b** in their article) as antiproliferative agents on Friend murine erythroleukemia (MEL) cells. They also reported that the cytotoxic activity of these compounds decreased after 48 h of incubation [19].

The IC_{50} values of **8b**, **8c**, **8d**, **9a**, **9b**, **9c**, and **9d** were 542.00 μM, 366.44 μM, 148.59 μM, 382.82 μM, 171.40 μM, 255.86 μM, and 140.60 μM, respectively (Table 1). It can be concluded that **9d**, **8d**, and **9b** have lower IC_{50} values. **8b** has the maximum IC_{50} at 542 μM.

In order to determine the relationship between the structures of the synthesized compounds and their anticancer activity, it would be rational to classify these compounds into two main groups: (i) The substituted groups bonded to the nitrogen atom of the imide. There are three different groups bonded to the nitrogen atom. These are benzyl, ethyl/metyl and phenyl groups. (ii) The substituted groups bonded to any atom of the cyclohexane ring. For this purpose, two derivatives were prepared for each group bonded to the nitrogen atom. These are 1-acetoxy-2-chlorocylohexane (**9a-d**) (Scheme3) and 1,4-diacetoxy cyclohexane derivatives (**8b-d**) (Scheme 2). A total of seven derivatives were prepared. Looking more closely at the structures and IC_{50} values of the first group (**9a**, **9b**, **9c**, and **9d**), **9d** (with the lowest IC_{50}) has a benzyl group, **9b** has an ethyl group, 9c has a phenyl group, and **9a** has a methyl group in their respective C(2)-positions. The order of IC_{50} values is **9d** < **9b** < **9c** < **9a**. According to these results we may suggest that as the -R group in the C(2)-position branches, the IC_{50} values decrease. In the second group, **8d** has a benzyl group, **8c** has a phenyl group, and **8b** has an ethyl group in their respective C(2)-positions. The order of IC_{50} values is **8d** < **8c** < **8b,** which also respect to the attached the group to nitrogen atom.

Table 1
Structure of drugs as a group with their IC_{50} values.

GROUP 1	IC_{50}	GROUP 2	IC_{50}
9a	382.82 μM	8b	542.00 μM
9b	171.40 μM	8c	366.44 μM
9c	255.86 μM	8d	148.59 μM
9d	140.60 μM		

The results were obtained using the GraphPad Prism 6 software program [20].

On analysis of this data, it could broadly be concluded that, most active compounds were derivatives of benzyl and ethyl groups on nitrogen atom compared to compounds are derivatives of phenyl group on nitrogen atom against HeLa cells. It seems phenyl group on nitrogen atom does not assist the compounds for improvement of anticancer activity. On the other hand, as seen from the table, the groups attached to the cyclohexane ring act more effective on the anticancer activity. The effect of 1-acetoxy-2-chlorocyclohexane derivatives **9b** was better than the effect of 1,4-diacetoxy cyclohexane derivatives **8b** against HeLa cells. This is clear evident when the 1-acetoxy-2-chlorocyclohexane derivative of the ethyl group is attached to the nitrogen atom, compared to the 1,4-diacetoxycyclohexane derivative. In addition, the methyl group was replaced with the ethyl group and the activity was determined to decrease.

In summary, in case of HeLa cells, excellent anticancer activity was noticed by three compounds **8d**, **9b** and **9d**. It was interesting to note that the electron-donating groups such as benzyl and ethyl substituent which is to bonded nitrogen atom may be responsible for the improvement of anticancer activity against HeLa cells. Cytotoxic effect was found to be greater when benzyl group was attached to nitrogen atom.

2.3. Western Blot analysis

According to results of MTT assay **9d**, **8c**, **8d** and **9b** showed more antiproliferative effect on HeLa cells and to better understand their acting mechanism, their relation with autophagy, they were chosen for Western Blot analysis.

For western blot, Cell Cignalling Phospho-p70 S6 Kinase (Thr389) (108D2) Rabbit mAb 9234, Phospho-p70 S6 Kinase (Ser371) Antibody 9208, Phospho-4E-BP1 (Thr37/46) (236B4) Rabbit mAb 2855 proteins were investigated. For primary and secondary antibody, Anti-rabbit IgG, HRP-linked Antibody 7074 and ß-Actin (13E5) rabbit mAb were chosen.

Two SDS-PAGE gel were performed for 3 protein, Beta Actin, p-4EBP1 and p-p70S6K. First gel imaging shows that the phosphorylated level of 4E-BP1 was overexpressed for the cells which were treated with **9d**, **8c** and **8d**, while control group and **9b** had approximately same protein level. Overexpression order is **9d**, **8c** and **8d**. It is known that if

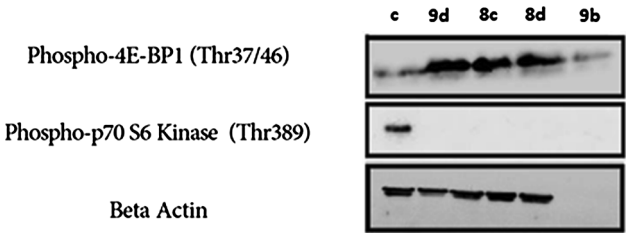

Fig. 3. Imaging of Gel 1.

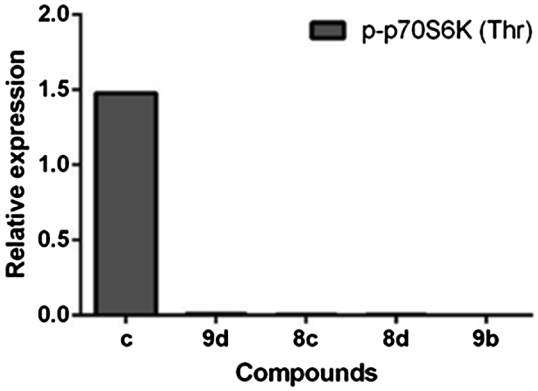

Fig. 4. Relative Expression of p-p70S6K (Thr).

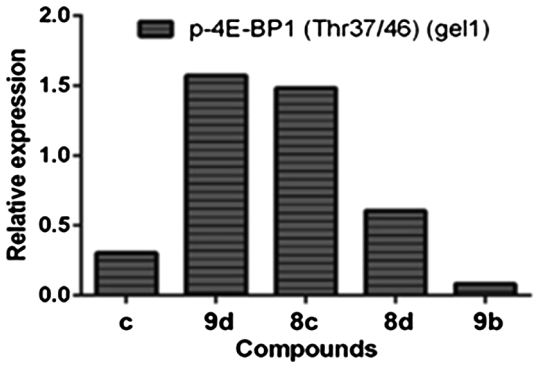

Fig. 5. Relative Expression of p-4E-BP1 (gel 1).

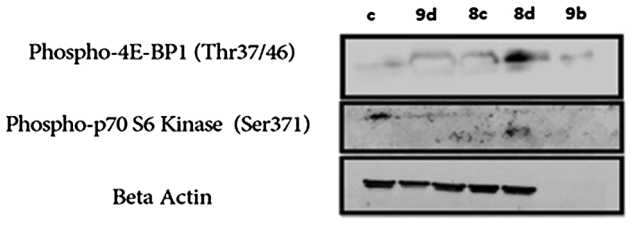

Fig. 6. Imaging of Gel 2.

mTOR inhibited, 4E-BP1 should overexpressed according to their inversely proportional relation (Figs. 3 and 6). Besides this, there were significant inhibition for phosphorylated level of p70S6K (Thr) protein, suggesting there were mTOR inhibition in the cells treated with these four drugs according to the direct proportional relation with mTOR and p70S6K (Figs. 3 and 6). Figs. 4 and 5 are quantification of the bands in the gel 1.

For the second gel, p-4EBP1 and p-p70S6K (Ser) antibodies were used. It was observed that there were overexpression of phosphorylated level of 4EBP1 protein for the cells treated with **9d**, **8c** and **8d** (in order of overexpression) according to untreated control group. Also, significant inhibiton for p-p70S6K (Ser) level in cells treated with these

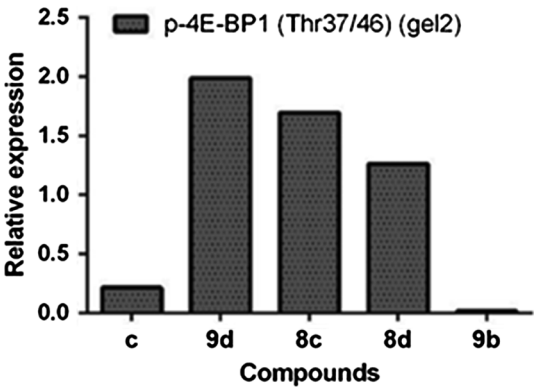

Fig. 7. Relative Expression of p-4E-BP1 (gel 2).

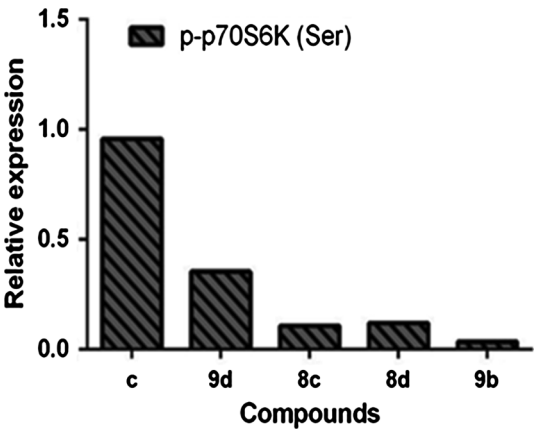

Fig. 8. Relative Expression of p-p70S6K (Ser).

four drugs according to control group were observed. Because of the high exposure time, there was high background for p-p70S6K (Ser) membrane. Figs. 7 and 8 are quantification of gel 2.

For the phosphorylated form of the 4EBP1, **9d** and **8c** had the maximum overexpressive effect, while they both inhibited the phosphorylated form of p70S6K (Thr). By looking the effects of each drug on protein levels, it might be a potent inhibitor. In a study published on 2016 suggest that 1-(2-hydroxy-5-methylphenyl)-3-phenyl-1,3-propanedione inhibits HeLa cell growth by causing a G1 arrest and by concomitantly inducing autophagy through the mediation of AMPK-mTOR and Akt-mTOR pathways, and may be a promising antitumor agent against cervical cancer [21]. Overall these findings suggest that drugs may inhibit cervical cancer cell proliferation by repressing the mTOR pathway.

2.4. Molecular modelling studies

Human mTOR and ribozomal S6 kinase β1 (RS6Kβ1) have been investigated as possible targets for compound series **8** and **9** (Table 1). To this end, crystal structures of human mTOR (pdb: 4jt5; 3.45 Å) and human RS6Kβ1 (pdb: 4l3j; 2.1 Å), both in complex with an inhibitor, were retrieved from the RCSB Protein DataBank (www.rcsb.org) [22].

Docking studies indicated that only compound **8c** may be able to bind to human mTOR (Fig. 9). Compound **8c** forms hydrogen bonds to the side chain of Lys2187 and the backbone of Val2240. The phenyl group of the ligand is within cation-π interaction distance (~3.5 Å) from the side chain of Lys2187 and it also forms an arene-H interaction with Ile2356. A benzyl or ethyl group at this position disturbs these binding interactions. Compound series **9** have a different scaffold with different relative orientations of the acetyl group with respect to the five-membered ring. In addition, it has a chlorine substituent. The

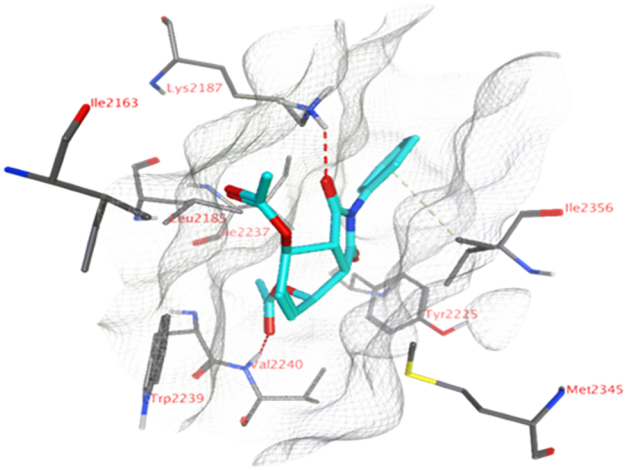

Fig. 9. The docked pose of compound **8c** (turquoise) in the binding pocket of human mTOR. Hydrogen bonds are indicated in red dashed lines, arene-H interactions are indicated in yellow dashed lines and the surface of the binding pocket is indicated with a white mesh.

structural changes also make the observed docked pose difficult to adopt in the mTOR binding pocket.

Docking studies into the active site of human RS6Kβ1 indicated that three different binding poses may be possible (Fig. 10). Compound **8d** forms hydrogen bonds to the side chains of Lys100 and Lys218 and an arene-H interaction between the ligand's phenyl group and the side chain of Leu74. The two carbonyl groups of the pyrrolidine-2,5-dione moiety do not form any interactions to the active site, but may form hydrogen bonds to the surrounding solvent. Compound **9d** also forms a hydrogen bond to the side chain of Lys100 and a second hydrogen bond to the backbone of Leu152. The second carbonyl group of the pyrrolidine-2,5-dione moiety does not form interactions with the protein but it is solvent exposed. Finally, compound **9d** also forms hydrogen bonds to the side chains of Lys100 and Lys218. All ligands form hydrophobic interactions with the active site.

3. Conclusions

Here we have reported an efficient synthesis of new derivatives of isoindole-1,3-dione bearing chloro/acetoxy groups at the 1,2-position of the cyclohexane ring. This method has the potential to be widely used in chloro- and acetoxy-substituted isoindole synthesis. The cytotoxic activities of these compounds were then evaluated in HeLa cells. Based on the results of the study, we suggest that all the newly synthesized isoindole derivatives might be good potential anticancer agents for the treatment of cervical cancer due to their antiproliferative activities in cancer cells. Molecular modelling studies suggested that human mTOR and ribozomal S6 kinase β1 (RS6Kβ1) may act as possible targets for compound series 8 and 9 and that these new derivatives of isoindole-1,3-dione may inhibit cervical cancer cell proliferation by repressing the mTOR pathway. However, the cytotoxic properties of these compounds should be thoroughly investigated in vitro and in vivo in detail for potential clinical utilization. Furthermore, the synthesis and activities of alternative isoindole derivatives are currently under investigation.

4. Experimental

4.1. Materials

All reagents used were commercially available unless otherwise specified and all solvents were distilled before use. Melting points were measured with Gallenkamp melting point devices. IR spectra: PerkinElmer Spectrum One FT-IR spectrometer. ^{1}H and ^{13}C NMR spectra: Varian 400 MHz and Bruker 400 MHz spectrometers. Elemental analysis results were obtained on a LECO CHNS-932 instrument.

5. Chemistry part

5.1. Synthesis of 3a,4,7,7a-tetrahydro-4,7-epoxyisobenzofuran-1,3-dione (6)

The synthesis was carried out following the literature procedure. [14–16]. In a 250-mL three-neck round-bottom flask under argon atmosphere, maleic anhydride (5.0 g, 50.99 mmol) and furan (5.2 g, 76.5 mmol) were dissolved in 20 mL of CH_2Cl_2. The mixture was stirred for 24 h while heating under reflux. A white precipitate formed during this time. The solid was collected by filtration and washed two times with cold diethyl ether. The filtrate was reduced by rotary evaporation to 20 mL and cooled to 4 °C overnight. A second crop crystallized, which was again collected by filtration and washed with diethyl ether. Finally, the crystals were dried in a vacuum ($\approx 10^{-2}$ mbar) overnight.

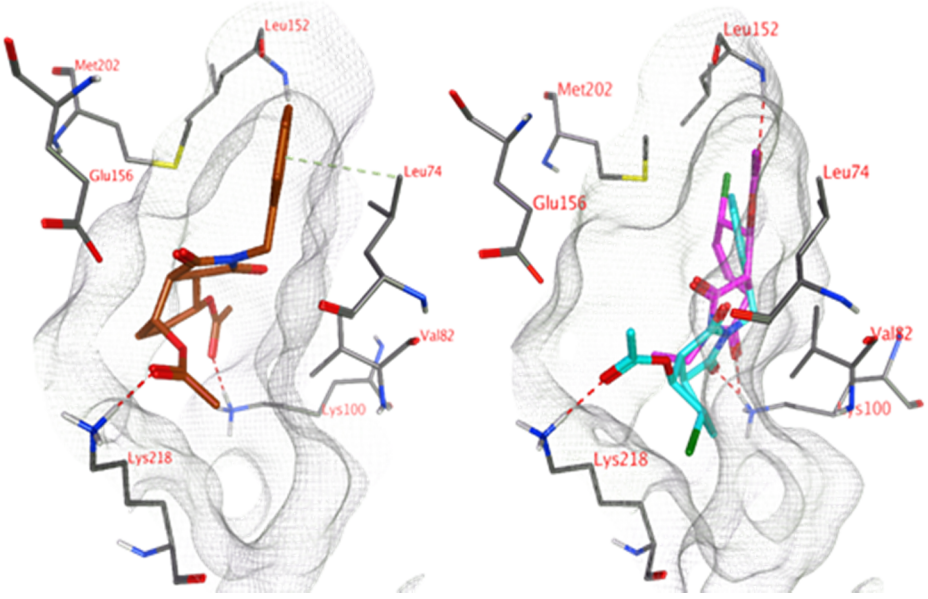

Fig. 10. The docked poses of compound **8d** (panel A; brown) and compounds **9b** and **9d** (panel B; purple and turquoise, respectively) in the binding pocket of human RS6Kβ1. Hydrogen bonds are indicated in red dashed lines, arene-H interactions are indicated in yellow dashed lines and the surface of the binding pocket is indicated with a white mesh.

Yield: 8.22 g (97%) of a white solid. ^{1}H NMR (400 MHz, $CDCl_3$) δ 6.57 (s, 2H, H_5, H_6), 5.45 (s, 2H, H_4, H_7), 3.18 (s, 2H, H_{3a}, H_{7a}). ^{13}C NMR (100 MHz, $CDCl_3$) δ 170.1 (2 CO), 137.2 (C_5, C_6), 82.4 (C_4, C_7), 48.9 (C_{3a}, C_{7a}).

5.2. General procedure for the synthesis of 4,7-epoxyisoindole-1,3(2H)-dione derivatives **7a-d**

The synthesis of 4,7-epoxyisoindole-1,3(2*H*)-dione derivatives started with 3a,4,7,7a-tetrahydro-4,7-epoxyisobenzofuran-1,3-dione (1.50 g, 9.03 mmol) (**6**). Compound **6** was dissolved in MeOH (15 mL) and primary alkyl/aryl amine (9.03 mmol) was added to the solution. It was refluxed in an oil bath for 24 h, and then it was cooled to room temperature and the crude product began to crystallize. It was put into a refrigerator overnight and the precipitate was filtered off. It was washed with hexane to give isoindole-1,3-dione derivatives 7**a-d**.

5.3. Methyl-3a,4,7,7a-tetrahydro-1H-4,7-epoxyisoindole-1,3(2H)-dione (**7a**)

Yield: 82% colorless crystals, M.p: 138–140 °C, ^{1}H NMR (400 MHz, $CDCl_3$) δ 6.49 (m, 2H, H_5, H_6), 5.24 (m, 2H, H_4, H_7), 2.94 (s, 3H, CH_3), 2.83 (s, 2H, H_{3a}, H_{7a}). ^{13}C NMR (100 MHz, $CDCl_3$) δ 176.5 (2xCO of imide), 136.7 (C_5 and C_6), 81.0 (C_4 and C_7), 47.7 (C_{3a} and C_{7a}), 25.1 (CH_3). Anal. Calcd. for $C_9H_9NO_3$: C, 60.33; H, 5.06; N, 7.82. Found: C, 60.68; H 4.91; N 7.66.

5.4. 2-Ethyl-3a,4,7,7a-tetrahydro-1H-4,7-epoxyisoindole-1,3(2H)-dione (**7b**)

Yield**:** 90% White powder, M.p.:119–121 °C. ^{1}H NMR (400 MHz, $CDCl_3$) δ 6.49 (s, 2H), 5.23 (s, 2H), 3.50 (q, J = 7.2 Hz, 2H), 2.81 (s, 2H), 1.13 (t, J = 7.2 Hz, 3H). ^{13}C NMR (100 MHz, $CDCl_3$) δ 176.30, 136.77, 81.09, 47.64, 34.09, 13.14. Anal. Calcd. for $C_{10}H_{11}NO_3$: C, 62.17; H, 5.74; N, 7.25. Found: C, 61.63; H, 5.87; N, 7.45.

5.5. 2-Phenyl-3a,4,7,7a-tetrahydro-1H-4,7-epoxyisoindole-1,3(2H)-dione (**7c**)

Yield: 55% Yellow crystalline solid, M.p.:134–136 °C. ^{1}H NMR (400 MHz, $CDCl_3$) δ 7.45–7.28 (m, 5H), 6.54 (s, 2H), 5.37 (s, 2H), 2.98 (s, 2H). ^{13}C NMR (100 MHz, $CDCl_3$) δ 175.63, 136.93, 131.93, 129.39, 129.03, 126.81, 81.65, 47.77 Anal. Calcd. for $C_{14}H_{11}NO_3$: C, 69.70; H, 4.60; N, 5.81. Found: C, 69.77; H, 4.72; N, 5.77.

5.6. 2-Benzyl-3a,4,7,7a-tetrahydro-1H-4,7-epoxyisoindole-1,3(2H)-dione (**7d**)

Yield**:** 54% White crystalline solid. M.p.:130–132 °C. ^{1}H NMR (400 MHz, $CDCl_3$) δ 7.29 (m, 5H), 6.47 (s, 2H), 5.25 (s, 2H), 4.62 (s, 2H), 2.82 (s, 2H). ^{13}C NMR (100 MHz, $CDCl_3$) δ 176.17, 136.79, 135.72, 128.86, 128.30, 128.00, 81.15, 47.75, 42.64. Anal. Calcd. for $C_{15}H_{13}NO_3$: C, 70.58; H, 5.13; N, 5.49. Found: C, 70.60; H, 5.27; N, 5.86.

5.7. Acid-catalyzed acetolysis of 7 with Ac_2O: the synthesis of 1,4-diacetoxy derivatives **8a-d**

Compounds **8a-d** were synthesized as described previously [14]. Isoindole derivative **7a** (1.0 g, 3.98 mmol) was dissolved in Ac_2O (5 mL). After the addition of 3 drops of H_2SO_4, the reaction mixture was magnetically stirred at room temperature for 2 days. Ac_2O was removed under reduced pressure. The crude product was recrystallized from CH_2Cl_2/hexane to give 1,4-diacetate derivatives **8a-d**.

5.8. 2-Methyl-1,3-dioxo-2,3,3a,4,7,7a-hexahydro-1H-isoindole-4,7-diyl-diacetate (**8a**)[14]

Yield**:** 82%. Colorless crystals, M.p.: 135–137 °C. ^{1}H NMR (400 MHz, $CDCl_3$) δ 6.26 (dm, J = 10.0 Hz, 1H, H_6) 6.01 (m, 1H, H_5), 5.34 (m, 1H, H_7), 5.16 (t, J = 4.8 Hz, 1H, H_4), 3.49 (bs, 2H, H_{3a}, H_{7a}), 2.96 (s, 3H, N-CH_3), 2.03 (s, 3H, C_7-OAc), 1.91 (s, 3H, C_4-OAc). ^{13}C NMR (100 MHz, $CDCl_3$) δ 175.5 (C_1), 175.2 (C_3), 169.6 (C_4-OAc), 169.2 (C_7-OAc), 126.6 (C_6), 125.2 (C_5), 67.0 (C_7), 64.3 (C_4), 40.0 (C_{7a}), 39.6 (C_{3a}), 25.1 (N-CH_3), 21.0 ($COCH_3$), 20.8 ($COCH_3$). Anal. Calcd. for $C_{13}H_{15}NO_6$: C 55.51; H 5.38; N 4.98. Found: C 55.19; H 5.29; N 5.00.

5.9. 2-Ethyl-1,3-dioxo-2,3,3a,4,7,7a-hexahydro-1H-isoindole-4,7-diyl diacetate (**8b**)

Yield**:** 62%. White powder, M.p.: 141–143 °C. ^{1}H NMR (400 MHz, $CDCl_3$) δ 6.32 (m, 1H, H_6), 6.06 (m, 1H, H_5), 5.38 (m, 1H, H_7), 5.18 (quasi t, J = 4.8 Hz, 1H, H_4), 3.55 (q, J = 7.1 Hz, 2H, *N*-CH_2), 3.46 (m, 2H, H_{3a}, H_{7a}), 2.05 (s, 3H, C_7-OAc), 1.93 (s, 3H, C_4-OAc), 1.15 (t, J = 7.2 Hz, 3H, N-CH_2**CH_3**). ^{13}C NMR (100 MHz, $CDCl_3$) δ 175.36, 174.97, 169.57, 169.20, 126.92, 124.97, 67.01, 64.07, 39.83, 39.45, 34.14, 20.99, 20.78, 13.24. Anal. Calcd. for $C_{14}H_{17}NO_6$: C, 56.95; H, 5.80; N, 4.74. Found: C, 56.40; H, 5.73; N, 4.67.

5.10. 1,3-Dioxo-2-phenyl-2,3,3a,4,7,7a-hexahydro-1H-isoindole-4,7-diyl diacetate (**8c**)

Yield 63%. Pale yellow solid. M.p.: 162–164 °C. ^{1}H NMR (400 MHz, $CDCl_3$) δ 7.51–7.24 (m, 5H), 6.42 (dd, J = 10.1, 3.5 Hz, 1H, H_6), 6.14 (m, 1H, H_5), 5.50 (quasi t, J = 4.2 Hz, 1H, H_7), 5.28 (quasi t, J = 4.8 Hz, 1H, H_4), 3.68 (m, 2H, H_{3a}, H_{7a}), 2.09 (s, 3H, C_7-OAc), 2.00 (s, 3H, C_4-OAc).^{13}C NMR (100 MHz, $CDCl_3$, ppm) δ 174.5, 174.32, 169.56, 169.13, 131.76, 129.53, 129.06, 126.76, 126.32, 125.13, 67.23, 63.95, 39.84, 39.72, 21.01, 20.96. Anal. Calcd. for $C_{18}H_{17}NO_6$: C, 62.97; H, 4.99; N, 4.08. Found: C, 62.47; H, 5.07; N, 4.04.

5.11. 2-Benzyl-1,3-dioxo-2,3,3a,4,7,7a-hexahydro-1H-isoindole-4,7-diyl diacetate (**8d**)

Yield 57%. White solid. M.p.: 92–94 °C. ^{1}H NMR (400 MHz, $CDCl_3$) δ 7.43–7.24 (m, 5H), 6.33 (dd, J = 10.0, 2.9 Hz, 1H, H_6), 6.04 (m, 1H, H_5), 5.36 (quasi t, J = 4.0 Hz, 1H, H_7), 5.11 (quasi t, J = 4.0 Hz, 1H, H_4), 4.63 (dd, J_{AB} = 14.0, 5.5 Hz, 2H, N-CH_2), 3.48 (m, 2H, H_{3a}, H_{7a}), 2.04 (s, 3H, C_7-OAc), 1.39 (s, 3H, C_4-OAc). ^{13}C NMR (100 MHz, $CDCl_3$) δ 175.28, 174.84, 169.45, 169.16, 135.87, 129.44, 128.88, 128.22, 127.01, 124.69, 66.46, 63.86, 42.77, 39.64, 39.42, 20.89, 19.96. Anal. Calcd. for $C_{19}H_{19}NO_6$: C, 63.86; H, 5.36; N, 3.92. Found: C, 63.64; H, 5.17; N, 3.92.

5.12. General procedure for the synthesis of 1,2-chloroacetate derivatives **9a-d**

In a round-bottom flask, tricyclic compounds **7a-d** (0.5 g) were dissolved with 4 mL of Ac_2O and then 2 mL of AcCl was added to this slurry solution at 25 °C. After that, three drops of H_2SO_4 were added drop by drop. After that addition, the color of the reaction began to darken. The resulting solution was stirred for 48 h. The reaction was concentrated under vacuum and unreacted AcCl was removed. The crude product was precipitated and the liquid layer was concentrated under vacuum. It was crystallized from CH_2Cl_2/hexane to give 1,2-chloroacetate derivatives **9a-d**.

5.13. 5-Chloro-2-methyl-1,3-dioxo-2,3,3a,4,5,7a-hexahydro-1H-isoindol-4-yl acetate (**9a**)

Yield 67%. Colorless crystal, M.p.: 89–91 °C. ^{1}H NMR (400 MHz, $CDCl_3$, ppm): δ 6.28 (dd, J = 9.9, 3.7 Hz, 1H, A part of AB system, H_6),

6.02 (m, 1H, B part of AB system, H_7), 5.47 (quasi t, J = 4.1 Hz, 1H, H_4) 4.47 (dd, J = 5.6, 3.5 Hz, 1H, H_5), 3.68 (dd, J = 8.9, 4.4 Hz, 1H, H_{3a}), 3.51 (dt, J = 8.8, 3.3 Hz, 1H, H_{7a}), 2.98 (s, 3H, C_4-OAc), 1.90 (s, 3H, N-CH_3). ^{13}C NMR (100 MHz, $CDCl_3$, ppm): δ 175.50, 175.36, 169.13, 125.81, 125.57, 69.19, 48.30, 39.28, 39.01, 25.09, 20.71. Anal. Calcd. for $C_{11}H_{12}ClNO_4$: C, 51.27; H, 4.69; N, 5.44. Found: C, 50.98; H, 4.73; N, 5.40.

5.14. 5-Chloro-2-ethyl-1,3-dioxo-2,3,3a,4,5,7a-hexahydro-1H-isoindol-4-yl acetate (**9b**)

Yield 58%, pale yellow solid. M.p.:105–107 °C. ^{1}H NMR (400 MHz, $CDCl_3$) δ 6.32 (dd, J = 9.9, 3.7 Hz, 1H, A part of AB system, H_6), 6.03 (m, 1H, B part of AB system, H_7), 5.50 (quasi t, J = 3.9 Hz, 1H, H_4), 4.50 (dd, J = 5.9, 3.3 Hz, 1H, H_5), 3.67 (dd, J = 9.0, 4.5 Hz, 1H, A part of AB system, H_{3a}), 3.58 (qd, J = 7.3, 1.5 Hz, 2H, N-CH_2), 3.50 (dt, J = 9.0, 3.3 Hz, 1H, B part of AB system, H_{7a}), 1.92 (s, 3H, C_4-OAc), 1.16 (t, J = 7.3 Hz, 3H, CH_3). ^{13}C NMR (100 MHz, $CDCl_3$) δ 175.30, 175.13, 169.26, 125.70, 125.66, 69.16, 47.97, 39.03, 38.52, 34.01, 20.53, 13.25. Anal. Calcd. for $C_{12}H_{14}ClNO_4$: C, 53.05; H, 5.19; N, 5.16. Found: C, 52.91; H, 5.19; N, 5.33.

5.15. 5-Chloro-1,3-dioxo-2-phenyl-2,3,3a,4,5,7a-hexahydro-1H-isoindol-4-yl acetate (**9c**)

Yield 60%, white solid. M.p.:125–127 °C. ^{1}H NMR (400 MHz, $CDCl_3$) δ 7.50–7.23 (m, 5H), 6.40 (dd, J = 9.8, 3.7 Hz, 1H, A part of AB system, H_6), 6.10 (m, 1H, B part of AB system, H_7), 5.59 (quasi t, J = 3.7 Hz, 1H, H_4), 4.57 (dd, J = 5.8, 3.3 Hz. 1H, H_5), 3.85 (dd, J = 9.2, 4.4 Hz, 1H, A part of AB system, H_{3a}), 3.72 (dd, J = 9.2, 3.3 Hz, 1H, B part of AB system, H_{7a}), 1.99 (s, 3H, C_4-OAc). ^{13}C NMR (100 MHz, $CDCl_3$) δ 174.45, 174.44, 169.11, 131.74, 129.56, 129.11, 126.32, 125.92, 125.43, 69.56, 48.09, 39.25, 38.97, 20.90. Anal. Calcd. for $C_{16}H_{14}ClNO_4$: C, 60.10; H, 4.41; N, 4.38. Found: C, 60.34; H, 4.61; N, 4.38.

5.16. 2-Benzyl-5-chloro-1,3-dioxo-2,3,3a,4,5,7a-hexahydro-1H-isoindol-4-yl acetate (**9d**)

Yield 51%, white solid. M.p: 81–83 °C. ^{1}H NMR (400 MHz, $CDCl_3$) δ 7.43–7.24 (m, 5H), 6.31 (dd, J = 9.9, 3.7 Hz, 1H, A part of AB system, H_6), 6.01 (m, 1H, B part of AB system, H_7), 5.44 (quasi t, J = 4.4 Hz, 1H, H_4), 4.63 (d, J_{AB} = 20.9 Hz, 2H, N-CH_2), 4.42 (dd, J = 5.9, 3.3 Hz, 1H, H_5), 3.66 (dd, J = 9.2, 4.4 Hz, 1H, A part of AB system, H_{3a}), 3.52 (dt, J = 9.2, 3.3 Hz, 1H, B part of AB system, H_{7a}), 1.37 (s, 3H, C_4-OAc). ^{13}C NMR (100 MHz, $CDCl_3$) δ 175.2, 174.9, 169.3, 135.8, 129.7, 129.0, 128.4, 125.7, 125.6, 68.9, 48.1, 43.0, 39.2, 38.7, 19.9. Anal. Calcd. for $C_{17}H_{16}ClNO_4$: C, 61.18; H, 4.83; N, 4.20. Found: C, 61.47; H, 4.93; N, 4.24.

6. Biological part

6.1. Cell cultures

HeLa cell lines were kindly provided by IZTECH Biotechnology and Bioengineering Research and Application Center, Izmir Institute of Technology, Turkey. Media for HeLa cells was Dulbecco's modified Eagle's medium (DMEM) (Sigma) with 4500 mg glucose/L, pyridoxine, HCl and $NaHCO_3$, without L-glutamine. HeLa cells were cultured in DMEM growth medium with 10% fetal bovine serum (Sigma), 10% penstrep solution (Biological Industries) and 10% L-glutamine solution (Biological Industries). Cells were incubated in an incubator which provides 37 °C and 5% CO_2. Medium was refreshed every 3 days for each cell culture. Typically, cells were passaged by trypsinization and in growth medium. All compounds were dissolved in dimethyl sulfoxide (DMSO) before all the analyses.

6.2. Cell viability assays

MTT (3-(4,5-Dimethylthiazol-2-yl)-2,5-diphenyltetrazolium bromide) proliferation assay was performed to evaluate the cytotoxicity of the synthesized norcantharimide compounds reflecting the cell viability of HeLa cell lines in presence of the compounds. MTT, a yellow tetrazole, is reduced to purple formazan in living cell's mitochondria by mitochondrial dehydrogenases of viable cells [20]. This reduction only occurs if mitochondrial reductase enzymes are active; thus, conversion is directly related to the number of viable cells. In the experiment, cells were cultured in 96-well plates (SPL Life Sciences) with 3x10^3 cell/well and waited for 24 h in order to attach surface of the plate bottom. Compounds were solved in sterile DMSO and stock solution of each seven compounds were prepared as 200 mM in 100 µl DMSO. Working concentrations were prepared by diluting that stock solutions with complete media and also DMSO (final DMSO concentration was 1% in a well) before the experiment. All compounds were added to wells according to 20, 50, 100, 200, 500, 1000, 2000 µM with triplicate assay. After all compound added, cells were incubated 24 h, 48 h and 72 h in order to determine cytotoxic effects. At the end of each incubation period, media was removed from wells and MTT stock solution (5 mg/ml PBS) was diluted 1:10 ratio with complete media and added to wells. After 4 h incubation, plates were centrifuged at 1800 rpm 10 min at room temperature. Supernatant was removed; DMSO was added to each well and shaked 150 rpm 15 min at room temperature in order to solve all formazan crystals. Absorbance was determined at 540 nm (Thermo Electron Type 1500 Multiskan Spectrum). Metabolic activity at standard growth conditions was considered as 100%. The concentration inhibiting cell viability by 50% (IC_{50} values) was calculated.

6.3. Western blot analysis

Whole cell protein extracts of compound treated HeLa cells were prepared using CelLytic™ MEM Protein Extraction Kit (Sigma). Cell Cignalling Phospho-p70 S6 Kinase (Thr389) (108D2) Rabbit mAb 9234, Phospho-p70 S6 Kinase (Ser371) Antibody 9208, Phospho-4E-BP1 (Thr37/46) (236B4) Rabbit mAb 2855 proteins were detected using primary and secondary antibody, Anti-rabbit IgG, HRP-linked Antibody 7074 and ß-Actin (13E5) rabbit mAb. The protein bands visualization was conducted using the Pierce™ ECL Western Blotting Substrate (Life Technologies) and a G:BOX imaging system.

6.4. Statistical analysis

The results represented the mean ± standard deviation from at least three independent experiments. Statistical significance was assessed by One-way ANOVA using GraphPad Prism 5, and with the Dunnett's multiple comparison tests.

6.5. Molecular modelling studies

The three-dimensional structures of all ligands were prepared in their lowest energy conformation using the MOE software package (v2019.01, Chemical Computing Group, Inc, Montreal, Canada) and the ligands were energy minimized (MMFF94x force field).

All protein structures were obtained from the RCSB protein databank: human mTOR in complex with inhibitor (pdb: 4jt5; 3.45 Å) and human RS6Kβ1 in complex with inhibitor (pdb: 4l3j; 2.1 Å). The protein and inhibitor atoms were retained and all other atoms were omitted. The remaining structure was protonated using the protonate 3D functionality of MOE and subsequently the obtained structure was energy-minimized (AMBER14:EHT) [23].

Docking calculations were performed using the FlexX docking tool (v2.3.2; BioSolveIT GmbH, St. Augustin, Germany) within MOE. The binding pocket was defined as all residues within 6.5 Å of the crystallized inhibitors. All ligands were docked fifty times and the best scoring

three poses were subjected to refinement calculations. To this end, the ligand and binding pocket residues were energy minimized and re-scored using GBVI/WSA force field [24].

Declaration of Competing Interest

We declare that we have no conflict of interest.

Acknowledgments

The authors would like to thank Atatürk University for financial support (Grant No: FCD-2018-7009 and FFM-2017-6349). The authors also thank the Biotechnology and Bioengineering Center laboratory staff of Izmir Institute of Technology and for its financial and technical support.

References

[1] N.S. El-Gohary, M.I. Shaaban, Synthesis, antimicrobial, antiquorum-sensing, and cytotoxic activities of new series of Isoindoline 1,3-dione, pyrazolo[5,1-a]- isoindole, and pyridine derivatives, Arch. Pharm. Chem. Life. Sci. 348 (2015) 666–680.

[2] C.E.P. Galvis, L.Y.V. Méndez, V.K. Kouznetsov, Cantharidin-based small molecules as potential therapeutic agents, Chem. Biol. Drug Des. 82 (2013) 477–499.

[3] P.F. Lamie, J.N. Philoppes, A.O. El-Gendy, L. Rarova, J. Gruz, Design, synthesis and evaluation of novel phthalimide derivatives as in vitro anti-microbial, anti-oxidant and anti-inflammatory agents, Molecules 20 (2015) 16620–16642.

[4] J.Y. Wu, C.D. Kuo, C.Y. Chu, M.S. Chen, J.H. Lin, Y.J. Chen, H.F. Liao, Synthesis of novel lipophilic N-substituted norcantharimide derivatives and evaluation of their anticancer activities, Molecules 19 (2014) 6911–6928.

[5] S.H.L. Kok, C.H. Chui, W.S. Lam, J. Chen, F.Y. Lau, R.S.M. Wong, G.Y.M. Cheng, P.B.S. Lai, T.W.T. Leung, Synthesis and structure evaluation of a novel cantharimide and its cytotoxicity on SK-Hep-1 hepatoma cells, Bioorg. Med. Chem. Lett. 17 (2007) 1155–1159.

[6] T.A. Hill, S.G. Stewart, S.P. Ackland, J. Gilbert, B. Sauer, J.A. Sakoff, A. McCluskey, Synthesis of new norcantharidin analogues and their anticancer evaluation, Bioorg. Med. Chem. 15 (2007) 6126–6134.

[7] P.Y. Lin, S.J. Shi, H.L. Shu, H.F. Chen, C.C. Lin, P.C. Liu, L.F. Wang, A simple procedure for preparationofN-thiazolyl and N-thiadiazolylcantharidinimides and evalution of their cytotoxicities against humanhepatocellular carcinoma cell, Bioorg. Chem. 28 (2000) 266–272.

[8] T.A. Hill, S.G. Stewart, B. Sauer, J. Gilbert, S.P. Ackland, J.A. Sakoff, A. McCluskey, Heterocyclic substituted cantharidin and norcantharidin analogues-synthesis, protein phosphatase (1 and 2A) inhibition and anticancer activity, Bioorg. Med. Chem.Lett. 17 (2007) 3392–3397.

[9] L.H. Lin, H.S. Huang, C.C. Lin, L.W. Lee, P.Y. Lin, Effects of cantharidins on human carcinoma cell Chem, Pharm. Bull 52 (2004) 855–857.

[10] A. McCluskey, C. Walkom, M.C. Bowyer, S.P. Ackland, E. Gardiner, J.A. Sakoff, Effects of cantharidins on human carcinoma cell, Bioorg. Med. Chem. Lett. 11 (2001) 2941–2946.

[11] J.A. Sakoff, S.P. Ackland, M.L. Baldwin, M.A. Keane, A. McCluskey, Anticancer activity and protein phosphatase 1 and 2A inhibition of a new generation of cantharidin analogues, Invest. New Drugs 20 (2002) 1–11.

[12] (a) A. Tan, B. Koc, E. Sahin, N.H. Kishali, Y. Kara, Synthesis of new cantharimide analogues derived from 3-sulfolene, Synthesis 7 (2011) 1079–1084;
(b) A. Tan, M.Z. Kazancioglu, D. Aktas, O. Gundogdu, E. Sahin, N.H. Kishali, Y. Kara, Convenient synthesis of new polysubstituted isoindole-1,3-dione analogues, Turk. J. Chem. 38 (2014) 629–637;
(c) A. Tan, E. Bozkurt, N.H. Kishali, Y. Kara, New and convenient synthesis of amino phthalimide derivatives and their photoluminescent properties, Helv. Chim. Acta 97 (2014) 1107–1114.

[13] A. Köse, Y. Bal, N.H. Kishalı, G. Sanlı-Mohamed, Y. Kara, Synthesis and anticancer activity evaluation of new isoindole analogues, Med. Chem. Res. 26 (2017) 779–786.

[14] Y.W. Goh, B.R. Pool, J.M. White, Structural studies on cycloadducts of furan, 2-methoxyfuran, and 5-trimethylsilylcyclopentadiene with maleic anhydride and N-methylmaleimide, Org. Chem. 73 (2008) 151–156.

[15] M. Sodeoka, Y. Baba, S. Kobayashi, N. Hirukawa, Structure-activity relationship of Cantharidin derivatives to protein phosphatases 1, 2A1, and 2B, Bioorg. Med. Chem. Lett. 7 (1997) 1833–1836.

[16] N.H. Kishali, E. Sahin, Y. Kara, Regio- and stereocontrolled synthesis of (2R*,3R*,4R*)-3,4-Dichloro-1,2,3,4,5,8-hexahydronaphthalen-2-yl acetate via tandem S_N2' reactions, Helv. Chim. Acta 89 (2006) 1246–1253.

[17] P. Mondal, S. Roy, G. Loganathan, B. Mandal, D. Dharumadurai, M.A. Akbarsha, P.S. Sengupta, S. Chattopadhyay, P.S. Guin, 1-Amino-4-hydroxy-9,10-anthraquinone - an analogue of anthracycline anticancer drugs, interacts with DNA and induces apoptosis in human MDA-MB-231 breast adinocarcinoma cells: evaluation of structure-activity relationship using computational, spectroscopic and biochemical studies, Biochem. Biophys. Rep. 4 (2015) 312–323.

[18] P. Lalitha, V. Veena, P. Vidhyapriya, P. Lakshmi, R. Krishna, N. Sakthivel, Anticancer potential of pyrrole (1, 2, a) pyrazine 1, 4, dione, hexahydro 3-(2-methyl propyl) (PPDHMP) extracted from a new marine bacterium, Staphylococcus sp. strain MB30, Apoptosis 21 (2016) 566–577.

[19] A. Mai, S. Massa, I. Cerbara, S. Valente, R. Ragno, P. Bottoni, R. Scatena‖, P. Loidl, G. Brosch, 3-(4-Aroyl-1-methyl-1H-2-pyrrolyl)-N-hydroxy-2-propenamides as a new class of synthetic histone deacetylase inhibitors. 2. Effect of pyrrole-C2 and/or -C4 substitutions on biological activity, J. Med. Chem. 47 (2004) 1098-1109.

[20] T.J. Mosmann, Rapid colorimetric assay for cellular growth and survival: application to proliferation and cytotoxicity assays, Immunol. Meth. 65 (1983) 55–63.

[21] J.H. Tsai, L.S. Hsu, H.C. Huang, C.L. Lin, M.H. Pan, H.M. Hong, W.J. Chen, 1-(2-Hydroxy-5-methylphenyl)-3-phenyl-1,3-propanedione induces G1 cell cycle arrest and autophagy in hela cervical cancer cells, Int. J. Mol. Sci. 17 (2016) 1274–1284.

[22] (a) H.M. Berman, J. Westbrook, Z. Feng, G. Gilliland, T.N. Bhat, H. Weissig, I.N. Shindyalov, P.E. Bourne, The Protein Data Bank, Nucleic Acids Res. 28 (2000) 235–242;
(b) H. Yang, D.G. Rudge, J.D. Koos, B. Vaidialingam, H.J. Yang, N.P. Pavletich, mTOR kinase structure, mechanism and regulation, Nature 497 (2013) 217–223;
(c) J. Wang, C. Zhong, F. Wang, F. Qu, J. Ding, Crystal structures of S6K1 provide insights into the regulation mechanism of S6K1 by the hydrophobic motif, Biochem. J. 454 (2013) 39–47.

[23] P. Labute, Protonate3D: assignment of ionization states and hydrogen coordinates to macromolecular structures, Proteins Struct. Funct. Bioinforma 75 (2009) 187–205.

[24] P. Labute, The generalized Born/volume integral implicit solvent model: Estimation of the free energy of hydration using London dispersion instead of atomic surface area, J. Comput. Chem. 29 (2008) 1693–1698.